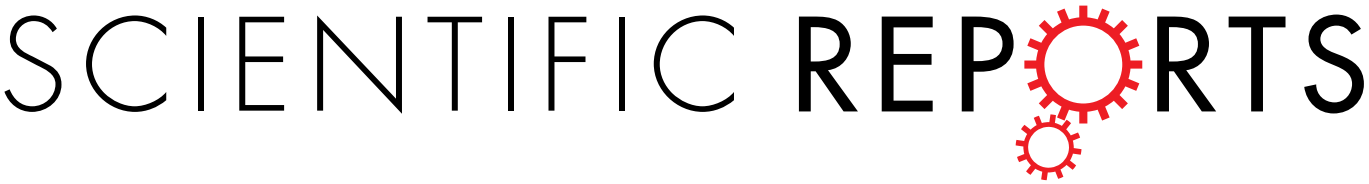

OPEN

Coherent backscattering in quasi-ballistic ultra-high mobility GaAs/AlGaAs 2DES

Received: 8 January 2018
Accepted: 21 June 2018
Published online: 03 July 2018

R. L. Samaraweera[1], H.-C. Liu[1], B. Gunawardana[1], A. Kriisa[1], C. Reichl[2], W. Wegscheider[2] & R. G. Mani[1]

A small and narrow negative-magnetoresistance (MR) effect that appears about null magnetic field over the interval $-0.025 \leq B \leq 0.025\ T$ in magnetotransport studies of the GaAs/AlGaAs 2D system with $\mu \approx 10^7 cm^2/Vs$ is experimentally examined as a function of the sample temperature, T. The temperature dependent magnetoresistance data were fit using the Hikami *et al*. theory, without including the spin-orbit correction, to extract the inelastic length, l_i, which decreases rapidly with increasing temperature. It turns out that $l_i < l_e$, where l_e is the elastic length, for all T. Thus, we measured the single particle lifetime, τ_s, and the single particle mean free path $l_s = v_F \tau_s$. A comparison between l_i and l_s indicates that $l_i > l_s$. The results suggest that the observed small and narrow magnetoresistance effect about null magnetic field could be a manifestation of coherent backscattering due to small angle scattering from remote ionized donors in the high mobility GaAs/AlGaAs 2DES.

Advancements in the molecular beam epitaxy growth of the GaAs/AlGaAs two dimensional electron system (2DES) now routinely yields high-quality heterostructures with 2D electron mobilities $\mu \geq 10^7\ cm^2/Vs$, making this the most disorder free 2D material system in existence. In such specimens, the transport or elastic length, $l_e = v_F(m^*\mu/e) = v_F\tau_e$, where v_F is the Fermi velocity, m^* is the effective mass, e is the charge, and τ_e is the transport/elastic time, can be comparable to the sample size even in mm-scale specimens, implying quasi ballistic transport in the absence of a magnetic field. Such high quality material has demonstrated new 2D physical phenomena such as the photo-excited zero-resistance states[1,2] and 1/4− cycle shifted magnetoresistance oscillations[3] induced by low energy photons in the low magnetic field, high filling factor limit. Associated results have produced new interest in the experimental[1–39] and theoretical[40–62] study of photo-excited transport in low dimensional systems. The dark properties of the GaAs/AlGaAs 2D material system in the low magnetic field limit have also attracted recent experimental attention as the results have helped to provide new insights into both an observable giant magnetoresistance in the 2DES, and a small, narrow negative magnetoresistance near null magnetic field[63–77]. So far as the latter effect is concerned[74,78,79], early reports[74] examined size effects and the phase-breaking rate of good quality GaAs/AlGaAs 2DES material from the 1980's, while in the lower mobility ($\approx 10^5\ cm^2V^{-1}s^{-1}$) 2DES[78,80,81], the temperature dependent conductivity drop at the null magnetic field was viewed as either localization or carrier interaction effect. In the modern era, Bockhorn *et al*. reported a temperature invariant small and narrow magnetoresistance effect around zero magnetic field as a sign for the absence of weak localization[82] in high quality GaAs/AlGaAs 2DES samples[71,73]. It turns out that the origin of the small and narrow negative magnetoresistance effect about null magnetic field in these ultra high mobility samples is still under debate since the low disorder and long elastic mean free path even in mm-scale high mobility GaAs/AlGaAs specimens suggests the absence of diffusive transport - a necessary condition for the observability of weak localization.

Quantum coherent backscattering originates from the constructive quantum interference of electronic wave-functions which return to the origin after propagating along time-reversed paths in a disordered diffusive medium[78,82–86]. This interference effects leads to enhanced carrier back-scattering and, therefore, to an increase in the resistivity above the classical Drude value. The observation of this interference effect requires that the inelastic length, l_i, exceed the elastic length, l_e, i.e., $l_i > l_e$. Since inelastic scattering events, such as electron-electron or electron-phonon interactions, and strong magnetic fields destroy the phase-coherence between time reversed trajectories, the quantum correction to the resistivity/conductivity becomes suppressed by higher temperatures,

[1]Department of Physics and Astronomy, Georgia State University, Atlanta, 30303, Georgia. [2]Laboratorium für Festkörperphysik, ETH Zürich, CH-8093, Zürich, Switzerland. Correspondence and requests for materials should be addressed to R.L.S. (email: marl@phy-astr.gsu.edu) or R.G.M. (email: rmani@gsu.edu)

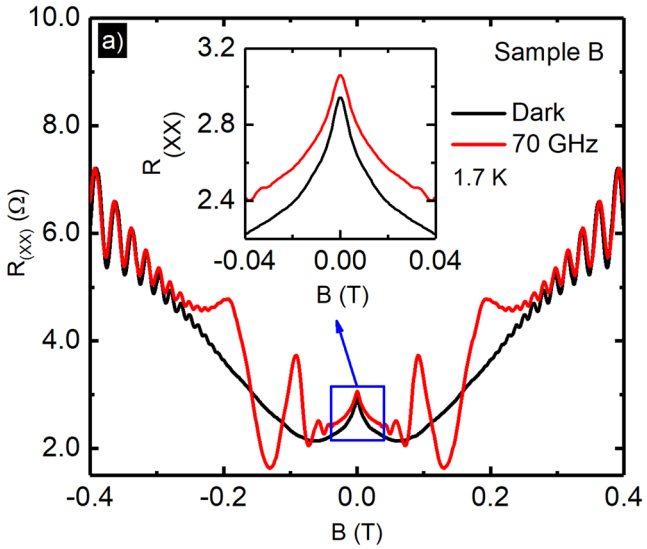

Figure 1. Radiation induced magnetoresistance oscillations in R_{xx} in a GaAs/AlGaAs heterostructure 2D electron system. R_{xx} is exhibited vs. the magnetic field, B, for dark (Black-curve) and with microwave excitation at $f = 70$ GHz and $P = 0.77\ mW$ (Red-curve). The inset shows the enlarged view of the weak localization-like effect.

or finite magnetic fields[82,83,85]. Typically, these interference effects are readily observable at low temperature as sharp magnetoresistance peak about $B = 0$.

Our magnetotransport studies have been characterized by two distinct negative magnetoresistance effects in the high quality GaAs/AlGaAs 2DES in the low magnetic field limit: (a) a negative Giant Magneto-Resistance (GMR) effect over larger magnetic fields ($-0.15 \leq B \leq 0.15\ T$) and (b) a small and narrow negative magnetoresistance effect in the immediate vicinity of null magnetic field. The dependence of the negative-GMR on the sample size, DC-bias, temperature, and also the interplay between GMR and the radiation induced magnetoresistance oscillations have been reported[72,76,87]. Here, we present the experimental study of the small and narrow negative magnetoresistance effect about $B = 0$. This effort represents an attempt (a) to determine whether a Hikami *et al.* theory[88] can succeed to model the small and narrow negative- magnetoresistance effect observed about $B = 0$ in the high mobility GaAs/AlGaAs 2D system, and (b) to extract characteristic parameters such as the inelastic length l_i. Thus, experimentally, we followed the small and narrow negative magnetoresistance effect as a function of the temperature, and the data were then fit using the Hikami *et al.* theory, neglecting spin-orbit interactions[88]. The results indicate that $l_i < l_e$ even at the lowest temperatures, while, typically, it is necessary that $l_i \geq l_e$ for weak localization. Since, in the high mobility GaAs/AlGaAs 2DES, small angle scattering from remote charged impurities predominates, and such scattering mostly influences the single particle scattering length, $l_s = v_F \tau_s$, rather than the elastic length l_e, we have also extracted τ_s from line-shape fits of Shubnikov-de Haas oscillations[89–91], and evaluated l_s. The results show that $l_i > l_s$, suggesting the possibility of a coherent backscattering effect that arises from small angle scattering due to remote charged impurities in the high mobility GaAs/AlGaAs system.

Results

Figure 1(a) exhibits magnetoresistance data (R_{xx}) obtained in the dark (black) and under photo-excitation (red) with microwaves at frequency, $f = 70\ GHz$ with a power level $P = 0.77\ mW$, at $T = 1.7\ K$. The inset of Fig. 1(a) exhibits an enlarged view of the small and narrow negative magnetoresistance effect, which is the main focus of this study. The small and narrow negative magnetoresistance term spans roughly over $-0.025 \leq B \leq 0.025\ T$, and it is reminiscent of the weak localization effect[72–74,79,82–84,86,92–95]. Note that the shape of the small and narrow negative magnetoresistance term is not significantly affected by the photo excitation, although the R_{xx} shifts to a higher value under photo-excitation. Figure 1 also indicates that the non-oscillatory portion of the data shows initial negative magnetoresistance to $B = 0.15\ T$, followed by positive magnetoresistance to $B = 0.35\ T$, with observable Shubnikov-de Haas oscillations for $B \geq 0.2\ T$.[24,27]. The radiation-induced magnetoresistance oscillations, can be observed roughly over the interval $-0.2 \leq B \leq 0.2\ T$ (red-curve)[1,3,5–12,14,15,18,20,24,27–30,32–34,36,39].

The above-mentioned small and narrow negative magnetoresistance effect is reported here on two samples, labeled sample-A and sample-B, with electron densities $n_A = 3.1 \times 10^{11}\ cm^{-2}$, $n_B = 2.4 \times 10^{11}\ cm^{-2}$ and electron mobilities $\mu_A = 1.37 \times 10^7\ cm^2/Vs$, $\mu_B = 1.13 \times 10^7\ cm^2/Vs$, respectively, over the temperature range $1.7 \leq T \leq 20.5\ K$. Figure 2(a) and (b) exhibit the raw magnetoresistivity data for the two samples at selected temperatures. The resistivity of the sample increases with increasing temperature as expected and the sample- A shows a much narrower negative magnetoresistance effect compared to the sample-B. In both samples, the FWHM of the peak increases with the increase of the temperature. We examined the small and narrow negative magnetoresistance effect using 2D weak localization theory.

In the absence of spin-orbit scattering, the 2D weak-localization correction to the resistivity is given by,

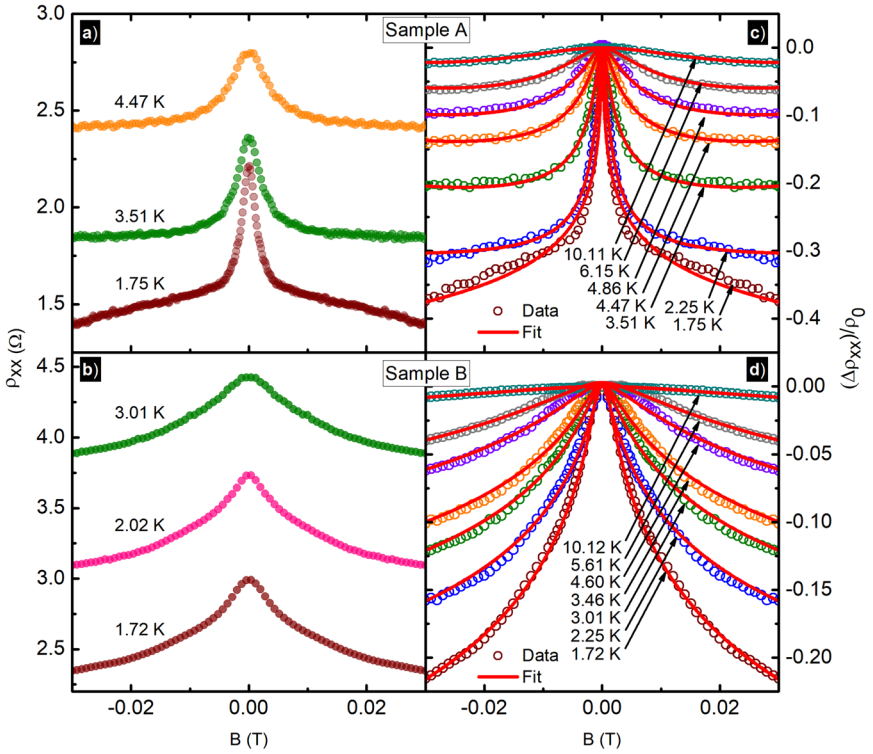

Figure 2. (**a**,**b**) These figures exhibit the magnetoresistivity data (ρ_{xx}) for sample-A and sample-B at selected temperatures, over the span of $-0.03T \leq B \leq 0.03T$. (**c**,**d**) The solid-circles exhibits the normalized experimental data ($\Delta\rho_{xx}/\rho_0$) vs B and solid-lines represent the corresponding fits using 2D weak localization theory.

$$\rho_{(B)} = \rho_{(0)} - \frac{e^2\rho^2}{2\pi^2\hbar}\left[\psi\left(\frac{1}{2} + \frac{B_i}{B}\right) + ln\frac{B}{B_i}\right] \tag{1}$$

Here, ψ is the digamma function, ρ resistivity, and

$$B_i = \frac{\hbar}{4el_i^2} \tag{2}$$

We fit the small and narrow negative magnetoresistance effect to equation (1) to extract l_i from the data[74,78,79,84,86,88,92,94,96]. Solid lines in Fig. 2(c) and (d) exhibit fits to the data of sample-A and sample-B respectively at selected temperatures. Note that the data and fit results in the Fig. 2(c) and (d) are shown as ($\Delta\rho_{xx}/\rho_0$) for the sake of clarity. Here, the maximum change in the resistivity ($\Delta\rho_{xx}/\rho_0$) due to the narrow negative-MR effect in sample-A at $T \approx 1.7\ K$ is ($\Delta\rho_{xx}/\rho_0$) = 0.37 and that of the sample-B is ($\Delta\rho_{xx}/\rho_0$) = 0.22. Thus, the small and narrow magnetoresistance effect is actually rather a substantial effect.

Figure 3(a) exhibits the temperature dependence of the inelastic length l_i for the sample-A (Blue) and sample-B (Red), calculated using the fit extracted parameter B_i. The l_i at the base temperature $T = 1.7\ K$ of the samples A and B are 4.10 μm and 0.76 μm, respectively, and l_i decreases monotonically with increasing temperature. In comparison, the elastic scattering length l_e for the samples-A and B are 123 μm and 79 μm respectively, and the characteristic width of the Hall bar sample is $W = 200\ \mu m$. Thus, the order of magnitude of W and l_e are the same although $W > l_e$. On the other hand, the $l_i \ll l_e$, roughly by a factor of 100. Sample-A with relatively higher electron density and mobility exhibits greater l_i and it differs from the sample-B by a factor of ≈ 5. The fit extracted l_i values of both samples follows T^{-2} law curves above $\approx 3\ K$, and data deviates from the curves showing a tendency of saturation at lower temperatures. The T^{-2} behavior of the l_i in the given temperature range suggests that the inelastic scatterings of these samples may be mainly electron-electron type[74,78,81,97]. Figure 3(b) exhibits the conductivity change, $\Delta\sigma$ as a function of the temperature for the two samples. Sample-A shows greater change in the conductivity for the small and narrow negative magnetoresistance effect. In both specimens, the small and narrow magnetoresistance effect becomes vanishingly small above $\approx 10K$. Note that the logarithmic temperature dependence of the conductivity correction in the low-temperature limit can be viewed as a signature of weak localization- effect in the 2DES[98,99].

As noted above, measurements suggest that $l_i < l_e$ in these quasi ballistic samples, which seems, at the outset, to rule out weak localization. However, it is known that small angle scattering from remote ionized impurities is predominant in the high mobility GaAs/AlGaAs 2D system and, as a consequence, the τ_e can exceed the single particle lifetime, τ_s, by factor of 100. (The τ_e reflects mostly large angle scattering while τ_s reflects all scattering,

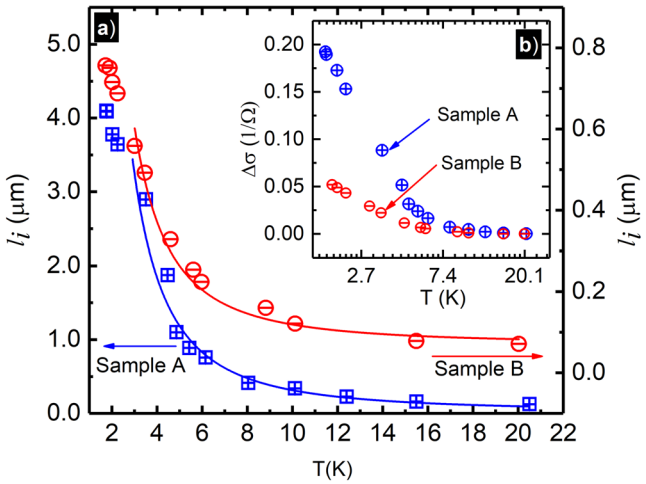

Figure 3. (**a**) This figure exhibits the temperature dependence of the inelastic scattering length l_i, for sample-A (Blue) and sample-B (Red), Solid lines correspond to T^{-2} law curves. Inset (**b**) shows $\Delta\sigma$ vs $Ln(T)$, $\Delta\sigma$ the localization-like correction to the Drude conductivity in 2D, sample-A (Blue) and sample-B (Red).

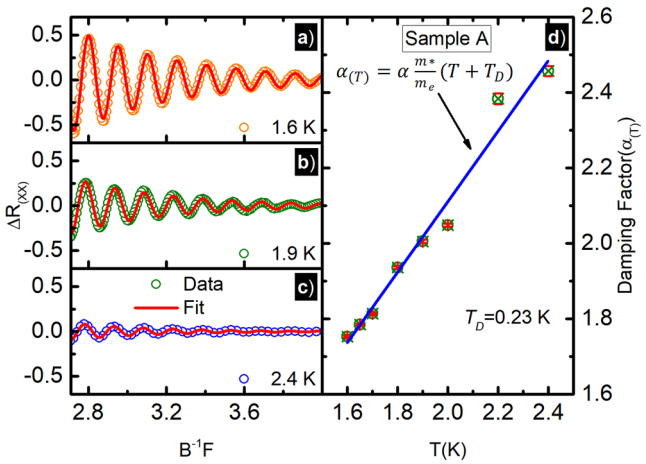

Figure 4. (**a**–**c**) This figures exhibit the background subtracted SdH-Oscillations, i.e. ΔR_{xx} vs $B^{-1}F$ (open circles) and numerical fit (red-solid lines) to equation (3), i.e. $\Delta R_{xx}^{fit} = A\ exp(-\alpha_{(T)}/B)cos(2\pi F/B)$, at different temperatures, F is the oscillations frequency and $\alpha_{(T)} = \alpha\, m^*/m_e(T + T_D)$ (see the text). (**d**) Exhibits the fit extracted temperature dependent damping factor $\alpha_{(T)}$ vs T for the sample-A.

including small angle scattering.) Thus, we utilized lineshape fits to determine the single particle lifetime τ_s, and thereby the single particle length, $l_s = v_F\tau_s$, which reflects all scattering events, from the low-field SdH oscillations[89–91]. Fig. 4(a–c) (open-circles) shows the SdH oscillations vs B^{-1}, scaled with oscillation frequency F for sample-A at some selected temperatures. Figure 4(a–c) red-solid lines exhibit the fit using equation (3).

$$\Delta R_{xx}^{fit} = A\ exp(-\alpha_{(T)}/B)cos(2\pi F/B) \tag{3}$$

Here, $\alpha_{(T)} = \alpha\ (m^*/m_e)(T + T_D)$, $\alpha = 14.69\ T/K$, $m^*/m_e = 0.064$ for these samples and T_D is the Dingle temperature. The intercept of the graph of $\alpha(T)$ vs T (i.e. Fig. 4(d)), determines the value of T_D. The τ_s is related to T_D through the expression $\tau_s = \hbar/2\pi k_B T_D$, where k_B is the Boltzmann constant. As shown in the Fig. 4(d), the calculated Dingle temperature for the sample-A is $T_D = 0.23 \pm 0.15K$ and the corresponding τ_s for the sample-A is $\tau_s = 4.86 \times 10^{-12}\ s$. Thus, for sample A, $l_s = v_F\tau_s = 1.26\,\mu m$, and $l_i > l_s$. This result suggests the possibility that the observed small and narrow negative magnetoresistance effect can be understood as coherent backscattering if small angle scattering due to remote ionized impurities is responsible for the scattering-induced closed electronic trajectories involved in weak localization.

Discussion

Magnetotransport studies of the ultra high mobility GaAs/AlGaAs 2DES exhibit a small and narrow negative magnetoresistance effect that appears around zero field[72,73,76,87]. This work aimed to follow the effect of temperature on the observed small and narrow negative magnetoresistance effect, determine whether a weak localization type line-shape analysis succeeds in describing the data, extract physical parameters, and possibly identify the physical origin of the observed effect. Thus, systematic measurements of the R_{xx} were carried out as a function of temperature ranging from 1.7 K to 20.5 K for two different samples and the data were fit using the Hikami 2D WL theory[88], neglecting the spin orbit scattering term, and also electron-electron interaction effects. The neglect of elecctron-electron interactions effects can be justified by the absence of an observable concurrent correction to the Hall coefficient[72].

With the increase of the temperature, the FWHM of the small and narrow negative-magnetoresistance effect increases and the peak height decreases, see Fig. 2(a,b), while it is restricted to weak magnetic fields around $B = 0$ T, see Fig. 1. This narrow peak is similar in appearance to the typical temperature dependent weak localization phenomena[78,82,85,92,100]. In canonical weak localization, the magnetoresistance effect disappears with increasing temperature as l_i, which initially exceeds l_e at the lowest temperatures, becomes smaller and, eventually, comparable with the elastic scattering length l_e, i.e., $l_i \approx l_e$. In both samples, the fit extracted inelastic length, l_i, see Fig. 3(a), monotonically decreases with increasing temperature. For the data shown here, in addition to the reduction in the inelastic scattering length with increased T, a result obtained through fits, quenching of the narrow negative-MR effect at higher temperatures is also confirmed by the reduced conductivity change $\delta\sigma$ with increasing T, see the inset of Fig. 3(b). A relatively stronger small and narrow negative-magnetoresistance effect is observed here in the sample A with the higher mobility/density. Figure 3(a) also indicates that the l_i in sample-A exceeds the l_i in sample-B throughout the examined temperature range. It is expected that a sample with higher mobility/density will exhibit a relatively larger l_i than a lower mobility/density sample[83].

The elastic scattering length l_e for the samples-A and B are 123 μm and 79 μm respectively, and the characteristic width of the Hall bar sample is $W = 200$ μm, i.e., the order of magnitude of W and l_e are the same although $W > l_e$. Thus, these specimens satisfy the quasi ballistic transport condition, while weak localization is a characteristic of diffusive transport. In these device structures, a high mobility of about $10^7 cm^2/Vs$ is achieved by utilizing the remote δ-doping technique. In this technique, scatterings due to ionized impurities are minimized while maintaining a higher electron concentration by separating the ionized impurities associated with donors from the 2D-electron layer[101,102]. In these high mobility specimens where scattering is predominantly due to long range Coulomb potentials from remote charged impurities, most scattering is expected to be of the small-angle variety. Since such scattering does not impact so much the transport time, one expects the elastic length, l_e, which is of the same order as the sample width, to not be the parameter of interest for comparison, as far as quantum coherent backscattering is concerned in this 2DES. Thus, we measured the single particle lifetime, τ_s, which tends to count all scattering, including small angle scattering, events. Figure 4 exhibits the evaluation of the temperature damping the SdH-oscillations that is used to calculate the τ_s and determine $l_s = v_F \tau_s$. Note that the ratio $l_e/l_s \approx 100$ in these specimens. This indicates that remote ionized impurity scattering, which favors small angle scattering, is predominant and significant in our samples, as reported by others for other modulation-doped GaAs/AlGaAs 2DES[89–91]. Therefore, we have reasoned that the criterion for the observability of coherent backscattering in such specimens is that $l_i > l_s$ holds true, rather than $l_i > l_e$, as is usual for weak localization. Indeed, it turns out that while $l_i > l_e$ is not satisfied in these specimens, the proposed alternate condition $l_i > l_s$ holds true. This feature has suggested the interpretation that the observed small and narrow negative magnetoresistance effect observed about zero magnetic field is coherent backscattering induced by small angle scattering from remote ionized impurities in the high mobility GaAs/AlGaAs 2DES.

A different explanation for this small and narrow negative-magnetoresistance effect around $B = 0$ in GaAs/AlGaAs 2DES has been given by Bockhorn *et. al.*[71,73]. Their measurements, carried out below $T = 800$ mK, exhibited a similar sharp negative-magnetoresistance effect around zero field that turned out, however, to be temperature independent. They suggested that the small and narrow negative magnetoresistance effect is induced both by rare strong scatters due to the presence of macroscopic defects and remote ionized impurities. In this regard, note that magnetoresistance saturation due to a saturation of the inelastic length at low temperatures, as $T \to 0$, is known[65,83].

Conclusions

In summary, this study examines a small and narrow-negative magneto resistance effect that appears around $B = 0$ T in the high mobility, $\mu \approx 10^7 cm^2/Vs$, GaAs/AlGaAs 2DES. This work reports the influence of sample temperature ($1.7 \leq T \leq 20$ K) and carrier density/mobility on the l_i, that are extracted using a Hikami *et al.* line-shape analysis[88]. The fit determined l_i decreases with increasing temperature, per expectations. The results indicate that $l_i < l_e$ at all temperatures, which is not what would be expected for canonical weak localization. However, since these specimens are characterized by charged impurity scattering from remote donors, scattering is expected to be predominantly of the small angle variety. Thus, we measured τ_s and l_s, the single particle lifetime and mean free paths, respectively, which take into account the small angle scattering. It turns out that $l_i > l_s$, which suggests the interpretation that the observed small and narrow negative magnetoresistance effect originates from coherent backscattering due to small angle scattering from remote ionized donors in the high mobility GaAs/AlGaAs 2DES.

Methods

High mobility MBE grown GaAs/AlGaAs heterostructures that consist of 5000 Å GaAs-substrate/100 × (100 Å AlGaAs | 30 Å GaAs)-Superlattice/12000 Å GaAs/700 Å AlGaAs/5 Å Si δ-doping/2400 Å AlGaAs/100 Å GaAs layers, were patterned into Hall bars by photolithography. The doping of the Si δ-layer is about $\approx 10^{12}$ cm^{-2}. Four terminal electrical measurements were carried out on the Hall bars using low-frequency lock-in based techniques

with the sample mounted at the end of a cylindrical waveguide, within a variable temperature insert, inside a superconducting solenoid in the $B \perp I$ configuration. Since the 200 μm wide Hall bars included voltage probes spaced by 200 μm, the effective Length-to-Width (L/W) ratio for the measurements presented here is L/W = 1. The samples were immersed in liquid helium, and temperature control was realized by controlling the vapor pressure of liquid helium. Typically, magnetic field (B) sweeps of the lock-in detected diagonal voltage V_{xx} were collected at a fixed temperature, T, in order to determine $R_{xx} = V_{xx}/I_{ac}$.

References

1. Mani, R. G. *et al.* Zero-resistance states induced by electromagnetic wave excitation in GaAs/AlGaAs heterostructures. *Nature* **420**, 646–650 (2002).
2. Zudov, M. A., Du, R. R., Pfeiffer, L. N. & West, K. W. Evidence for a new dissipationless effect in 2D electronic transport. *Phys. Rev. Lett.* **90**, 046807–1-4 (2003).
3. Mani, R. G. *et al.* Demonstration of a 1/4 cycle phase shift in the radiation-induced oscillatory-magnetoresistance in GaAs/AlGaAs devices. *Phys. Rev. Lett.* **92**, 146801-1-4 (2004).
4. Kovalev, A. E., Zvyagin, S. A., Bowers, C. R., Reno, J. L. & Simmons, J. A. Observation of a node in the quantum oscillations induced by microwave radiation. *Sol. St. Comm.* **130**, 379–381 (2004).
5. Mani, R. G. *et al.* Radiation induced oscillatory Hall effect in high mobility GaAs/AlGaAs devices. *Phys. Rev. B* **69**, 161306-1-4 (2004).
6. Mani, R. G. *et al.* Radiation induced zero-resistance states in GaAs/AlGaAs heterostructures: Voltage-current characteristics and intensity dependence at the resistance minima. *Phys. Rev. B* **70**, 155310-1-5 (2004).
7. Mani, R. G. *et al.* Radiation-induced oscillatory magnetoresistance as a sensitive probe of the zero-field spin splitting in high-mobility GaAs/AlGaAs devices. *Phys. Rev. B* **69**, 193304-1-4 (2004).
8. Mani, R. G. Zero-resistance states induced by electromagnetic-wave excitation in GaAs/AlGaAs heterostructures. *Physica E (Amsterdam)* **22**, 1–6 (2004).
9. Mani, R. G. Radiation-induced zero-resistance states with resolved Landau levels. *Appl. Phys. Lett.* **85**, 4962–4964 (2004).
10. Simovic, B., Ellenberger, C., Ensslin, K. & Wegscheider, W. Density dependence of microwave induced magnetoresistance oscillations in a two-dimensional electron gas. *Phys. Rev. B* **71**, 233303-1-4 (2005).
11. Mani, R. G. Radiation-induced oscillatory magnetoresistance in a tilted magnetic field in GaAs/AlGaAs devices. *Phys. Rev. B* **72**, 075327-1-5 (2005).
12. Mani, R. G. Photo-excited zero-resistance states in quasi-two-dimensional GaAs/AlGaAs devices. *Sol. St. Comm.* **144**, 409–412 (2004).
13. Smet, J. H. *et al.* Circular-polarization-dependent study of the microwave photoconductivity in a two-dimensional electron system. *Phys. Rev. Lett.* **95**, 116804-1-4 (2005).
14. Mani, R. G. Spin characterization and control over the regime of the radiation-induced zero-resistance states. *IEEE Trans. Nanotechnol.* **4**, 27–34 (2005).
15. Mani, R. G. Radiation-induced decay of Shubnikov-de Haas oscillations in the regime of the radiation-induced zero-resistance states. *Appl. Phys. Lett.* **91**, 132103-1-3 (2007).
16. Wirthmann, A. *et al.* Far-infrared-induced magnetoresistance oscillations in GaAs/AlGaAs-based two-dimensional electron systems. *Phys. Rev. B* **76**, 195315-1-5 (2007).
17. Studenikin, S. A. *et al.* Frequency quenching of microwave-induced resistance oscillations in a high-mobility two-dimensional electron gas. *Phys. Rev. B* **76**, 165321-1-6 (2007).
18. Mani, R. G. Narrow-band radiation-sensing in the Terahertz and microwave bands using the radiation-induced magnetoresistance oscillations. *Appl. Phys. Lett.* **92**, 102107-1-3 (2008).
19. Wiedmann, S. *et al.* Interference oscillations of microwave photoresistance in double quantum wells. *Phys. Rev. B* **78**, 121301-1-4 (2008).
20. Mani, R. G., Johnson, W. B., Umansky, V., Narayanamurti, V. & Ploog, K. Phase study of oscillatory resistances in microwave irradiated and dark GaAs/AlGaAs devices: Indications of an unfamiliar class of integral quantum Hall effect. *Phys. Rev. B* **79**, 205320-1-10 (2009).
21. Chepelianskii, A. D. & Shepelyansky, D. L. Microwave stabilization of edge transport and zero-resistance states. *Phys. Rev. B* **80**, 241308-1-4 (2009).
22. Wiedmann, S. *et al.* Magnetoresistance oscillations in multilayer systems: Triple quantum wells. *Phys. Rev. B* **80**, 245306-1-9 (2009).
23. Konstantinov, D. & Kono, K. Photon-induced vanishing of magnetoconductance in 2D electrons on liquid helium. *Phys. Rev. Lett.* **105**, 226801-1-4 (2010).
24. Mani, R. G., Gerl, C., Schmult, S., Wegscheider, W. & Umansky, V. Nonlinear growth with the microwave intensity in the radiation-induced magnetoresistance oscillations. *Phys. Rev. B* **81**, 125320-1-6 (2010).
25. Wiedmann, S., Gusev, G. M., Raichev, O. E., Bakarov, A. K. & Portal, J. C. Thermally activated intersubband scattering and oscillating magnetoresistance in quantum wells. *Phys. Rev. B* **82**, 165333-1-8 (2010).
26. Wiedmann, S., Gusev, G. M., Raichev, O. E., Bakarov, A. K. & Portal, J. C. Microwave zero-resistance states in a bilayer electron system. *Phys. Rev. Lett.* **105**, 026804-1-4 (2010).
27. Ramanayaka, A. N., Mani, R. G. & Wegscheider, W. Microwave induced electron heating in the regime of the radiation-induced magnetoresistance oscillations. *Phys. Rev. B* **83**, 165303-1-5 (2011).
28. Mani, R. G., Ramanayaka, A. N. & Wegscheider, W. Observation of linear-polarization-sensitivity in the microwave-radiation-induced magnetoresistance oscillations. *Phys. Rev. B* **84**, 085308-1-4 (2011).
29. Ramanayaka, A. N., Mani, R. G., Inarrea, J. & Wegscheider, W. Effect of rotation of the polarization of linearly polarized microwaves on the radiation-induced magnetoresistance oscillations. *Phys. Rev. B* **85**, 205315-1-6 (2012).
30. Mani, R. G., Hankinson, J., Berger, C. & de Heer, W. A. Observation of resistively detected hole spin resonance and zero-field pseudo-spin splitting in graphene. *Nature Commun.* **3**, 996, https://doi.org/10.1038/ncomms1986 (2012).
31. Konstantinov, D., Monarkha, Y. & Kono, K. Effect of coulomb interaction on microwave-induced magnetoconductivity oscillations of surface electrons on liquid helium. *Phys. Rev. Lett.* **111**, 266802-1-5 (2013).
32. Mani, R. G., Kriisa, A. & Wegscheider, W. Magneto-transport characteristics of a 2D electron system driven to negative magneto-conductivity by microwave photoexcitation. *Sci. Rep.* **3**, 3478, https://doi.org/10.1038/srep03478 (2013).
33. Mani, R. G. *et al.* Terahertz photovoltaic detection of cyclotron resonance in the regime of the radiation-induced magnetoresistance oscillations. *Phys.Rev. B* **87**, 245308-1-8 (2013).
34. Ye, T., Liu, H.-C., Wegscheider, W. & Mani, R. G. Combined study of microwave-power/linear polarization dependence of the microwave-radiation-induced magnetoresistance oscillations in GaAs/AlGaAs devices. *Phys. Rev. B* **89**, 155307-1-5 (2014).
35. Chepelianskii, A. D., Watanabe, N., Nasyedkin, K., Kono, K. & Konstantinov, D. An incompressible state of a photo-excited electron gas. *Nat. Comm.* **6**, 7210, https://doi.org/10.1038/ncomms8210 (2015).

36. Ye, T., Liu, H.-C., Wang, Z., Wegscheider, W. & Mani, R. G. Comparative study of microwave radiation-induced magnetoresistive oscillations induced by circularly- and linearly- polarized photoexcitation. *Sci. Rep.* **5**, 14880, https://doi.org/10.1038/srep14880 (2015).
37. Mani, R. G. Method for determining the residual electron- and hole- densities about the neutrality point over the gate-controlled n-p transition in graphene. *Appl. Phys. Lett.* **108**, 033507 (2016).
38. Herrmann, T. *et al*. Analog of microwave-induced resistance oscillations induced in GaAs heterostructures by terahertz radiation. *Phys. Rev. B* **94**, 081301-1-5 (2016).
39. Liu, H.-C., Samaraweera, R. L., Reichl, C., Wegscheider, W. & Mani, R. G. Study of the angular phase shift in the polarization angle dependence of the microwave induced magnetoresistance oscillations. *Phys. Rev. B* **94**, 245312-1-7 (2016).
40. Durst, A. C., Sachdev, S., Read, N. & Girvin, S. M. Radiation-induced magnetoresistance oscillations in a 2D electron gas. *Phys. Rev. Lett.* **91**, 086803-1-4 (2003).
41. Ryzhii, V. & Suris, R. Nonlinear effects in microwave photoconductivity of two-dimensional electron systems. *J. Phys.: Cond. Matt.* **15**, 6855–6869 (2003).
42. Andreev, A. V., Aleiner, I. L. & Millis, A. *J. Dynamical symmetry breaking as the origin of the zero-dc-resistance state in an ac-driven system. Phys. Rev. Lett.* **91**, 056803-1-4 (2003).
43. Koulakov, A. A. & Raikh, M. E. Classical model for the negative dc conductivity of ac-driven two-dimensional electrons near the cyclotron resonance. *Phys. Rev. B* **68**, 115324-1-4 (2003).
44. Lei, X. L. & Liu, S. Y. Radiation-induced magnetoresistance oscillation in a two-dimensional electron gas in Faraday geometry. *Phys. Rev. Lett.* **91**, 226805-1-4 (2003).
45. Rivera, P. H. & Schulz, P. A. Radiation-induced zero-resistance states: Possible dressed electronic structure effects. *Phys. Rev. B* **70**, 075314-1-6 (2004).
46. Dmitriev, I. A., Vavilov, M. G., Aleiner, I. L., Mirlin, A. D. & Polyakov, D. G. Theory of microwave-induced oscillations in the magnetoconductivity of a two-dimensional electron gas. *Phys. Rev. B* **71**, 115316-1-11 (2005).
47. Torres, M. & Kunold, A. Kubo formula for Floquet states and photoconductivity oscillations in a two-dimensional electron gas. *Phys. Rev. B* **71**, 115313-1-13 (2005).
48. Lei, X. L. & Liu, S. Y. Radiation-induced magnetotransport in high mobility two-dimensional systems: Role of electron heating. *Phys. Rev. B* **72**, 075345-1-10 (2005).
49. Inarrea, J. & Platero, G. Theoretical approach to microwave radiation-induced zero-resistance states in 2D electron systems. *Phys. Rev. Lett.* **94**, 016806-1-4 (2005).
50. Inarrea, J. & Platero, G. Temperature effects on microwave-induced resistivity oscillations and zero-resistance states in two-dimensional electron systems. *Phys. Rev. B* **72**, 193414-1-4 (2005).
51. Raichev, O. E. Magnetic oscillations of resistivity and absorption of radiation in quantum wells with two populated subbands. *Phys. Rev. B* **78**, 125304-1-14 (2008).
52. Inarrea, J. Effect of frequency and temperature on microwave-induced magnetoresistance oscillations in two-dimensional electron systems. *Appl. Phys. lett.* **92**, 192113-1-3 (2008).
53. Dmitriev, I. A., Khodas, M., Mirlin, A. D., Polyakov, D. G. & Vavilov, M. G. Mechanisms of the microwave photoconductivity in two-dimensional electron systems with mixed disorder. *Phys. Rev. B* **80**, 165327-1-9 (2009).
54. Inarrea, J., Mani, R. G. & Wegscheider, W. Sublinear radiation power dependence of photoexcited resistance oscillations in two-dimensional electron systems. *Phys. Rev. B* **82**, 205321-1-5 (2010).
55. Mikhailov, S. A. Theory of microwave-induced zero-resistance states in two-dimensional electron systems. *Phys. Rev. B* **83**, 155303-1-12 (2011).
56. Inarrea, J. Influence of linearly polarized radiation on magnetoresistance in irradiated two-dimensional electron systems. *Appl. Phys. Lett.* **100**, 242103-1-3 (2012).
57. Lei, X. L. & Liu, S. Y. Linear polarization dependence of microwave-induced magnetoresistance oscillations in high mobility two-dimensional systems. *Phys. Rev. B* **86**, 205303-1-5 (2012).
58. Iñarrea, J. Linear polarization sensitivity of magnetotransport in irradiated two-dimensional electron systems. *J. Appl. Phys.* **113**, 183717-1-5 (2013).
59. Zhirov, O. V., Chepelianskii, A. D. & Shepelyansky, D. L. Towards a synchronization theory of microwave-induced zero-resistance states. *Phys. Rev. B* **88**, 035410-1-14 (2013).
60. Raichev, O. E. Theory of magnetothermoelectric phenomena in high-mobility two-dimensional electron systems under microwave irradiation. *Phys. Rev. B* **91**, 235307-1-16 (2015).
61. Beltukov, Y. M. & Dyakonov, M. I. Microwave-induced resistance oscillations as a classical memory effect. *Phys. Rev. Lett.* **116**, 176801-1-5 (2016).
62. Chang, C.-C., Chen, G.-Y. & Lin, L. Dressed photon induced resistance oscillation and zero-resistance in arrayed simple harmonic oscillators with no impurity. *Sci. Rep.* **6**, 37763, https://doi.org/10.1038/srep37763 (2016).
63. Girvin, S. M., Jonson, M. & Lee, P. A. Interaction effects in disordered Landau-level systems in two dimensions. *Phys. Rev. B.* **26**, 1651–1659 (1982).
64. Houghton, A., Senna, J. R. & Ying, S. C. Magnetoresistance and Hall effect of a disordered interacting two-dimensional electron system. *Phys. Rev. B* **25**, 2196–2210 (1982).
65. Mani, R. G., von Klitzing, K. & Ploog, K. Magnetoresistance over the intermediate localization regime in GaAs/AlGaAs quantum wires. *Phys. Rev. B* **48**, 4571–4574 (1993).
66. Mani, R. G., von Klitzing, K. & Ploog, K. Localization at high magnetic fields in GaAs/AlGaAs quantum wires. *Phys. Rev. B* **15**, 9877–9880 (1992).
67. Mirlin, A. D., Polyakov, D. G., Evers, F. & Wolfle, P. Quasiclassical negative magnetoresistance of a 2D electron gas: Interplay of strong scatterers and smooth disorder. *Phys. Rev. Lett.* **87**, 126805-1-4 (2001).
68. Li, L., Proskuryakov, Y. Y., Savchenko, A. K., Linfield, E. H. & Ritchie, D. A. Magnetoresistance of a 2D electron gas caused by electron interactions in the transition from the diffusive to the ballistic regime. *Phys. Rev. Lett.* **90**, 076802-1-4 (2003).
69. Bykov, A. A., Zhang, J.-Q., Vitkalov, S., Kalagin, A. K. & Bakarov, A. K. Zero-differential resistance state of two-dimensional electron systems in strong magnetic fields. *Phys. Rev. Lett.* **99**, 116801-1-4 (2007).
70. Inarrea, J. Interplay of dc current and microwaves in the magnetotransport of two-dimensional electron systems. *Phys. Rev. B* **80**, 193302-1-4 (2009).
71. Bockhorn, L., Barthold, P., Schuh, D., Wegscheider, W. & Haug, R. *J. Magnetoresistance in a high mobility two-dimensional electron gas. Phys. Rev. B* **83**, 113301-1-4 (2011).
72. Mani, R. G., Kriisa, A. & Wegscheider, W. Size-dependent giant-magnetoresistance in millimeter scale GaAs/AlGaAs 2D electron devices. *Sci. Rep.* **3**, 2747, https://doi.org/10.1038/02747 (2013).
73. Bockhorn, L. *et al*. Magnetoresistance induced by rare strong scatterers in a high-mobility two-dimensional electron gas. *Phys. Rev. B* **90**, 165434-1-5 (2014).
74. Choi, K. K., Tsui, D. C. & Alavi, K. Dephasing time and one-dimensional localization of two-dimentional electrons in GaAs/AlGaAs heterostructures. *Phys. Rev. B* **15**, 36-7751-7754 (1987).
75. Inarrea, J. Theoretical model for negative giant magnetoresistance in ultra high mobility 2D electron systems. *Europhys. Lett.* **106**, 47005-1-5 (2014).

76. Wang, Z., Samaraweera, R. L., Reichl, C., Wegscheider, W. & Mani, R. G. Tunable electron heating induced giant magnetoresistance in the high mobility GaAs/AlGaAs 2D electron system. *Sci. Rep.* **6**, 38516, https://doi.org/10.1038/srep38516 (2016).
77. Inarrea, J., Bockhorn, L. & Haug, R. *J. Negative huge magnetoresistance in high mobility 2D electron gases: DC-current dependence. Europhys. Lett.* **115**, 17005-1-5 (2016).
78. Taboryski, R. & Lindelof, P. E. Weak localisation and electron-electron interaction in modulation-doped GaAs/AlGaAs heterostructures. *Semicond. Sci. Technol.* **5**, 933–946 (1990).
79. Englert Th. *et al*. Weak localization effect in GaAs doping superlattices. *Serf. Sci.* **142**, 68–72 (1984).
80. Poole, D. A., Pepper, M. & Glew, R. W. Electron-electron interaction in GaAs-AlGaAs heterostructures. *J.Phys. C: Solid State Phys.* **14**, L559–L1005 (1981).
81. Uren, M. J., Davies, R., Kaveht, M. & Pepper, M. Logarithmic corrections to two dimensional transport in silicon inversion layers. *J.Phys. C: Solid State Phys.* **14**, 5737–5762 (1981).
82. Bergmann, G. Weak localization in thin films - a time-of-flight experiment with conduction electrons. *Phys.Repts.* **107**, 1–58 (1984).
83. Ihn, T. Semiconductor Nanostructures and Electronic Transport in Nanostructures (ed. Ihn, T.) 265-286 (Oxford, 2010).
84. GrbiÄ‡, B., Leturcq, R., Ihn, T., Ensslin, K., Reuter, D., & Wieck, A., D. Strong spin-orbit interactions and weak antilocalization in carbon-doped p-type GaAsAlGaAs heterostructures. *Phys. Rev. B.* **77**, 125312-1-8 (2008).
85. Mani, R. G., Ghenim, L. & Choi, J. B. Weak localization in the narrow gap bulk semiconductors HgCdTe and InSb. *Solid State com.* **79**(No. 8), 693–697 (1991).
86. McPhail, S. *et al*. Weak localization in high-quality two-dimensional systems. *Phy. Rev. B* **70**, 245311-1-15 (2004).
87. Samaraweera, R. L. *et al*. Mutual influence between current-induced giant magnetoresistance and radiation-induced magnetoresistance oscillations in the GaAs/AlGaAs 2DES. *Sci. Rep.* **7**, 5074, https://doi.org/10.1038/s41598-017-05351-8 (2017).
88. Hikami, S., Larkin, A. I. & Nagoaka, Y. Spin-orbit interaction and magnetoresistance in the two-dimensional random system. *Prog. Theor. Phys.* **63**, 707–710 (1980).
89. Mani, R. G. & Anderson, J. R. Study of the single-particle and transport lifetimes in GaAs/AlGaAs. *Phys. Rev. B.* **137**, 4299–4302 (1988).
90. Elhamri, S. *et al*. AlGaN/GaN heterostructures: Effective mass and scattering times. *Phy. Rev. B* **57**(No. 3), 1374–1377 (1998).
91. Stoger, G. *et al*. Shubnikov-de Haas oscillations and negative magnetoresistance under hot-electrsn conditions in Si/SiGe heterostructures. *Semicond. Sci. Technol.* **9**, 765–771 (1994).
92. Tambasov, I. A. *et al*. Weaklocalization and size effects in thin In 2O3 films prepared by autowave oxidation. *Physica E.* **84**, 162–167 (2016).
93. Capoen, B., Biskupski, G. & Briggs, A. Low-temperature conductivity and weak-localization effect in barely metallic GaAs. *J. Phys. Cond. Matter* **5**, 2545–2552 (1993).
94. Lin, J. J. & Giordano, N. Electron scattering times from weak localization studies of Au-Pd films. *Phy. Rev. B* **35**(No. 3), 1071–1075 (1987).
95. Hansen, J. E., Taboryski, R. & Lindelof, P. E. Weak localization in GaAs heterostructures close to population of the second subband. *Phy. Rev. B* **47**(No. 23), 16040–16043 (1993).
96. McCann, E. *et al*. Weak localization magnetoresistance and Valley symmetry inGraphene. *Phy. Rev. Lett.* **97**, 16805-1-4 (2006).
97. Abrahams, E., Anderson, P. W., Lee, P. A. & Ramakrishnan, T. V. Quasiparticle lifetime in disordered two-dimensional metals. *Phys. Rev. B* **24**, 12-6783-6789 (1981).
98. Rammer, J. Quantum Transport Theory, 431–478, (Westview Press) (2004).
99. Gao, X. P. A. *et al*. Weak-Localization-Like Temperature-Dependent Conductivity of a Dilute Two-Dimensional Hole Gas in a Parallel Magnetic Field. *Phy. Rev. B* **89**(No. 1), 016801-1-4 (2002).
100. Senz, V. *et al*. Analysis of the Metallic Phase of Two-Dimensional Holes in SiGe in Terms of Temperature DependentScreening. *Phy. Rev. Lett.* **85**(No. 20), 4357–4360 (2000).
101. Umansky, U., de-Picciotto, R. & Heiblum, M. Extremely high-mobility two dimensional electron gas: Evaluation of scattering mechanisms. *Appl. Phys. Lett.* **71**(5), 683–685 (1997).
102. Dingle, R., Stormer, H. L., Gossard, A. C. & Wiegmann, W. Electron mobilities in modulation-doped semiconductor heterojunction superlattices. *Appl. Phys. Lett.* **33**(7), 665–667 (1978).

Acknowledgements

This work was supported by the Army Research Office under W911NF-14-2-0076 and W911NF-15-1-0433, the U.S. Department of Energy, Office of Basic EnergySciences, Material Science and Engineering Division under DE-SC0001762, and the NSF under ECCS1701302.

Author Contributions

Measurements were carried out by R.L.S. Experimental development, data modeling, and manuscript by R.L.S. and R.G.M. Technical support for cryogenic measurements was provided by H-C.L. B.G. and A. K. contributed to the fitting discussions. High quality GaAs/AlGaAs wafers are due to C.R. and W.W.

Additional Information

Competing Interests: The authors declare no competing interests.

Publisher's note: Springer Nature remains neutral with regard to jurisdictional claims in published maps and institutional affiliations.